





Mechanical Properties of a Stainless Steel after Annealing in Uranium Carbide

Yüksel Sarıkaya¹ , Müşerref Önal^{1*} , Abdullah Devrim Pekdemir² 

¹Ankara University, Department of Chemistry, Ankara, Turkey

²Ankara University, Graduate School of Natural and Applied Sciences, Ankara, Turkey

Abstract: The aim of this study was to investigate the interaction of carbide nuclear fuels with steel that is being used as cladding material for nuclear reactors. The specimens prepared from steel EN 1.4988 were consecutively annealed in three uranium carbide (UC) powders, having different carbon contents, at 600 °C for 1000 h. Both Ar and Na were used as bonding elements. The increase in the carbon content of the carburized specimens was determined and evaluated according to the bound and free carbon contents in the UC powders. The migration of free and bound carbon atoms into steel via self-diffusion and over Fe₃C formation is interpreted as carburizing. Microhardness measurements and stress-strain tests were used to determine the mechanical properties of crude and carburized steel specimens. Maximum hardness at the contact surface and depth of the carburized zone were determined from the microhardness profiles and discussed depending on the bonding elements and carbon content in the specimens. These variables have a significant impact on the elongation percent, 0.2% yield stress, and tensile stress.

Keywords: Carburizing, mechanical properties, microhardness, stainless steel, uranium carbide

Submitted: March 21, 2022. **Accepted:** August 22, 2022.

Cite this: Sarıkaya Y, Önal M, Pekdemir A. Mechanical Properties of a Stainless Steel after Annealing in Uranium Carbide. JOTCSA. 2022;9(4):1035-46.

DOI: <https://doi.org/10.18596/jotcsa.1090922>.

***Corresponding author. E-mail:** onal@science.ankara.edu.tr.

INTRODUCTION

Austenitic stainless steel, including trace amounts of free carbon atoms, is an alloy with different compositions. A large number of machine components are being made from stainless steel due to their excellent metallurgical, mechanical, and physicochemical properties. Also, they are extensively being used for the construction of nuclear fuel clads. Plutonium-uranium oxide or carbide are used as nuclear fuels (1). The out-of-pile test revealed that the physicochemical effect of oxide fuels on clads is larger than that of carbide ones. Since they have the same chemical properties, nonactive uranium carbide powders are being used instead of real carbide fuels. Carburizing processes are also carried out at elevated temperatures, either by tempering of steels or by reaction among several carbonaceous mediums such as kerosene, methanol, and carbon nanotubes (2-4). Carbon atoms diffused into steel are supplied from a carbonaceous medium (5-7). The depth of the

hardened diffusion layer in steel is determined by the measurement of carbon content or microhardness profiles as well as optical or electron microscopical images (8-10). Carburizing kinetics of various steels are studied using both of these profiles (11-14).

Besides carburizing, other types of corrosion have an effect on the mechanical properties of steels such as hardness, elongation percent, yield stress, ultimate tensile stress, ductility, fracture stress, and wear resistance (15-17). Mechanical properties of hardening steels following carburizing or different thermal and coating treatments are investigated (18-21). The effect of machining induced surface residual stress on the micro crack density of a steel was examined (22). Oxide and carbide films formed on the surface of the steels are characterized (23-25). The effect of annealing temperature and time on steel plasma carburization has previously been studied (26-28). Although such studies exist, the effect of the free and bound carbon content of the

carburizer as well as the bonding types of elements on the mechanical properties of steel is not yet sufficiently examined. Therefore, the aim of this study is to evaluate the change in carbon content, carburized depth, elongation percent, 0.2% yield stress, and tensile stress of a stainless steel depending on the uranium carbide powders that are being proposed as nuclear fuels.

MATERIAL AND METHODS

Materials

EN 1.4988 satinless steel with 1 mm thickness was used in this study as cladding material. The chemical composition of the crude steel is given as mass %: Fe 69.90; Cr 16.10; Ni 13.60; Mo 1.28; Mn 1.10; Ta+Nb 0.87; V 0.70; Si 0.27; C 0.08; Co 0.06; P 0.02; S 0.01 and N trace. Three uranium carbide (UC) powders with different compositions, indicated as UC(1), UC(2), and UC(3) were used as carburizers (Table 1). These powders also contain uranium oxide, uranium nitride, and free carbon as impurities. Due to the pyrophoric property of UC, all carburizing processes were performed under argon atmosphere in a glove box.

Table 1: Chemical composition (mass%) of the uranium carbide powders.

Powders	U	C	C (free)	O	N
UC(1)	95.105	4.820	-	0.037	0.038
UC(2)	94.786	4.960	0.034	0.170	0.050
UC(3)	94.654	5.150	0.053	0.120	0.023

Experimental

All four steel specimens were placed into six steel capsules at equal depths and distances (Figure 1). All the starting UC(1), UC(2), and UC(3) powders were placed into two capsules and vibration was applied to cover the specimens. Then, liquid sodium was added in one of the identical two capsules. After being tightly closed, each capsule was inserted into silica tubes and evacuated to 10^{-4} mmHg, then

sealed off. Silica tube assembly was heated in a muffle furnace for 1000 hours at 600 °C. Working temperature is selected as 600 °C being the maximum working temperature of nuclear reactors. They were removed after the furnace cooled. The crude steel and carburized specimens were marked as S0, S1, S2, and S3, respectively, according to their UC numbers.

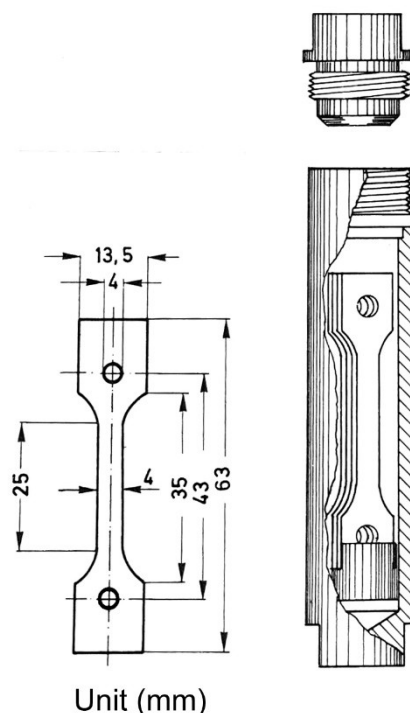


Figure 1: Dimension of steel specimens and their positions in the capsule tree.

Carbon content of the carburized specimens in each capsule was determined by converting it to carbon dioxide at high temperature. Specimens taken from each capsule were cut perpendicular to the contact

surface. The cross section surfaces were respectively polished and etched for microscopic examination and microhardness measurements. The Vickers microhardness gradients were measured

with a Leitz Durimet machine using an indentation load of 100 g. Room temperature elongation percent, 0.2% yield stress, and tensile stress for crude and carburized steel specimens were calculated using stress-strain curves plotted by a commercial testing machine.

RESULTS AND DISCUSSION

Surface Morphology

The microstructure of the cross-section surface of the carburized specimen UC(1) by argon bonding

was given in Figure 2. There is a clear distinction between carburized and unaffected regions on the cross-section surfaces. Different metal carbides such as Fe_3C and $Cr_{23}C_6$ (29,30) formed as carburizing precipitates on the grain boundaries in the form of thick lines (Figure 2). Iron carbide (Fe_3C : cementite) is the major component of the heterogeneous solid mixture (31-36). Bonded carbon atoms in UC were migrated into the steel after the formation of Fe_3C , while free carbon impurities in UC powder would be migrated via both Fe_3C formation and self-diffusion.

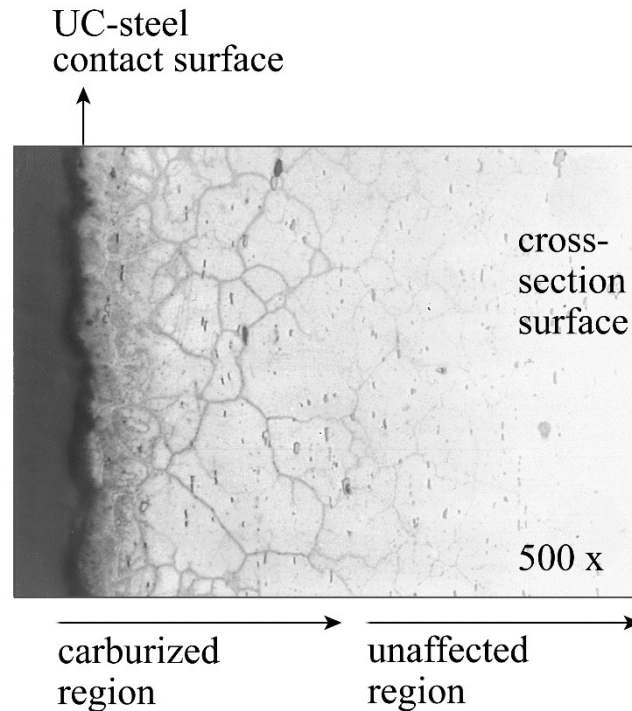


Figure 2: Optical micrographs of the cross-section surface of a specimen carburized in UC(1) by Ar-bonding.

Hard and brittle cementite was formed through the reversible reaction:



Temperature dependence of Gibbs free energy (free enthalpy change) for this reaction is given in SI units as follows

$$\Delta G^0 = \Delta H^0 - T \Delta S^0 = 26694 - 24.769T \quad (\text{Eq. 2})$$

Where ΔH^0 and ΔS^0 are the change in enthalpy and entropy, respectively (33). Since $\Delta H^0 > 0$, the reaction is endothermic. Based on Le Châtelier's principle, Fe_3C becomes more stable compared to Fe and C with increasing temperature. The carburizing process observed in the interior walls of the steel was explained by this reaction. Since crude or carburized steel is a heterogeneous mixture of Fe, C, and Fe_3C , the ratio among these components has a significant effect on the mechanical properties of steel.

Increasing Carbon Content in the Steel by Carburizing

The effect of carburizing on the physicochemical and mechanical properties of steel changes depending on the chemical composition of steel and carbon content as well as the annealing temperature, heating and cooling rate, and bonding properties. In this study, we have investigated the carbon content and bonding properties. The variation in carbon content of steel through Ar- and Na-bonding along with the carbon content of uranium carbide are given in Table 2 and represented in Figure 3. This variation depends on the total and free carbon content in the uranium carbon powders as well as the bonding materials used. The increase in the carbon content of steel by Na-bonding is greater than that of Ar-bonding. Also, free carbon atoms into the powder diffuse in the steel more effectively. According to the basic laws of thermodynamics, carbon atoms spontaneously move from a high chemical potential state to a low one. The effect of

carbon content on the mechanical properties of the steel is discussed in the section below.

Table 2: Mechanical properties of the crude and carburized steel samples.

Steels	C %	h_s (VH)	x_{max} (μm)	Elongation (%)	0.2% Yield strength (N/mm ²)	Tensile strength (N/mm ²)
S0	0.08	210	0	54	270	540
S1-Ar	0.19	500	180	24	292	618
S1-Na	0.21	500	180	24	315	585
S2-Ar	0.26	600	220	12	410	635
S2-Na	0.27	600	220	7.5	440	615
S3-Ar	0.30	705	300	10	410	668
S3-Na	0.59	705	300	2	470	685

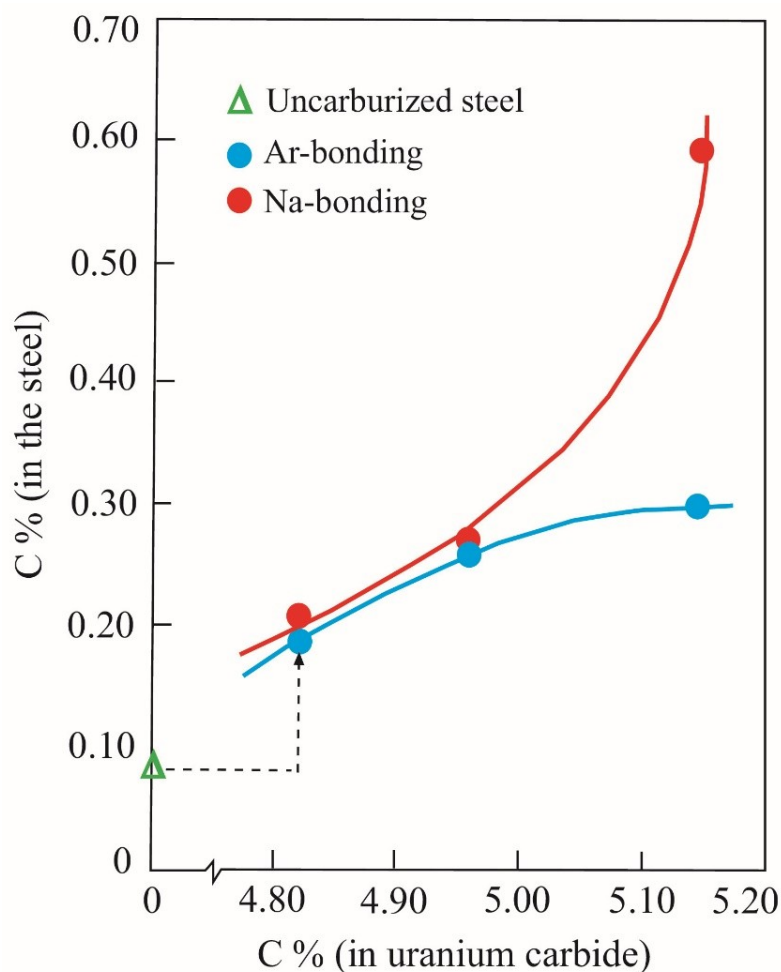


Figure 3: Variation of the carbon content in the steel with the carbon content in the uranium carbide powder.

Microhardness Profiles

Vickers microhardness profiles on the cross-section of the carburized specimens in UC(1), UC(2), and UC(3) by Ar- and Na- bonding are represented in Figure 4, Figure 5, and Figure 6, respectively. Here, h_0 is the microhardness of the uncarburized steel, h_s is the maximum microhardness at the nearest distance to the contact surface, and x_m is the

maximum depth of the carburized region. The corresponding microhardness profiles by the Ar- and Na-bonding are overlapped for the specimens carburized in UC(1) and UC(2), while different than those in UC(3). This difference is due to the excess free carbon atoms in the UC(3) carried faster by sodium bonding. Although the results vary considerably depending on the physicochemical

properties of the materials and carburizing study generally agree with the literature data conditions (25,26,29,31,35), the outcomes of this (17,19,36).

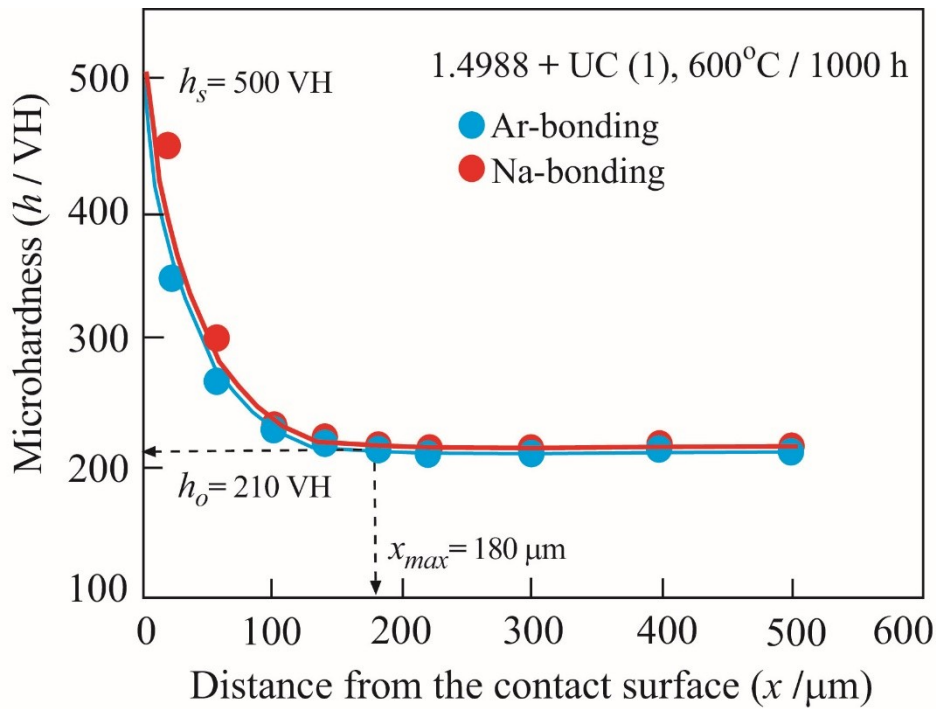


Figure 4: Microhardness profiles for the specimens carburized in UC(1) by the Ar-bonding and Na-bonding.

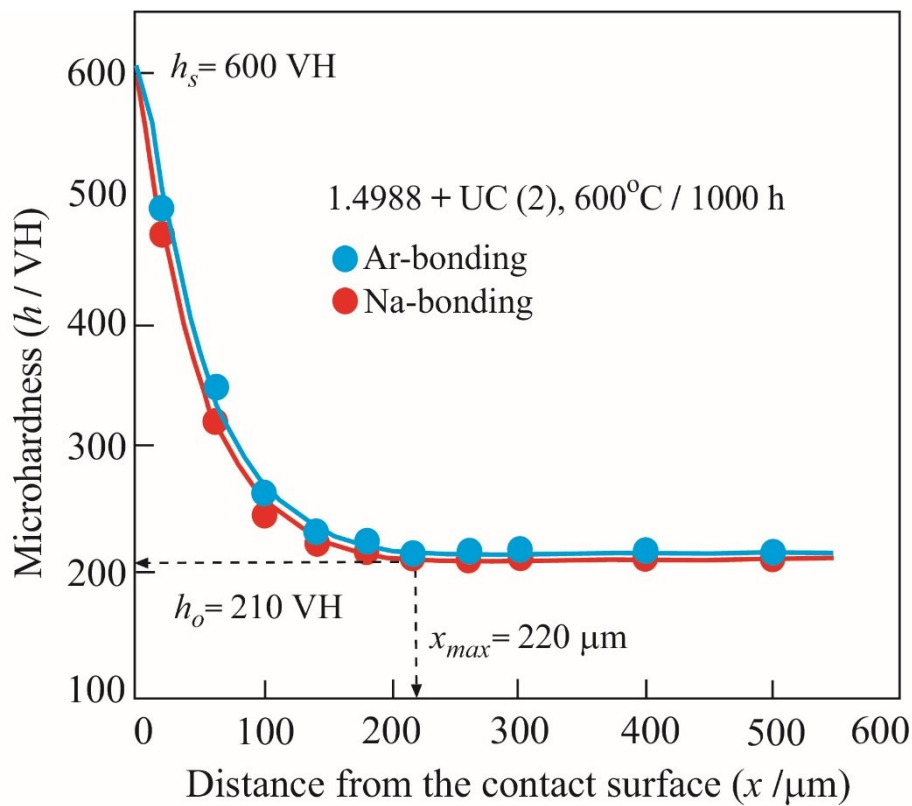


Figure 5: Microhardness profiles for the specimens carburized in UC(2) by the Ar-bonding and Na-bonding.

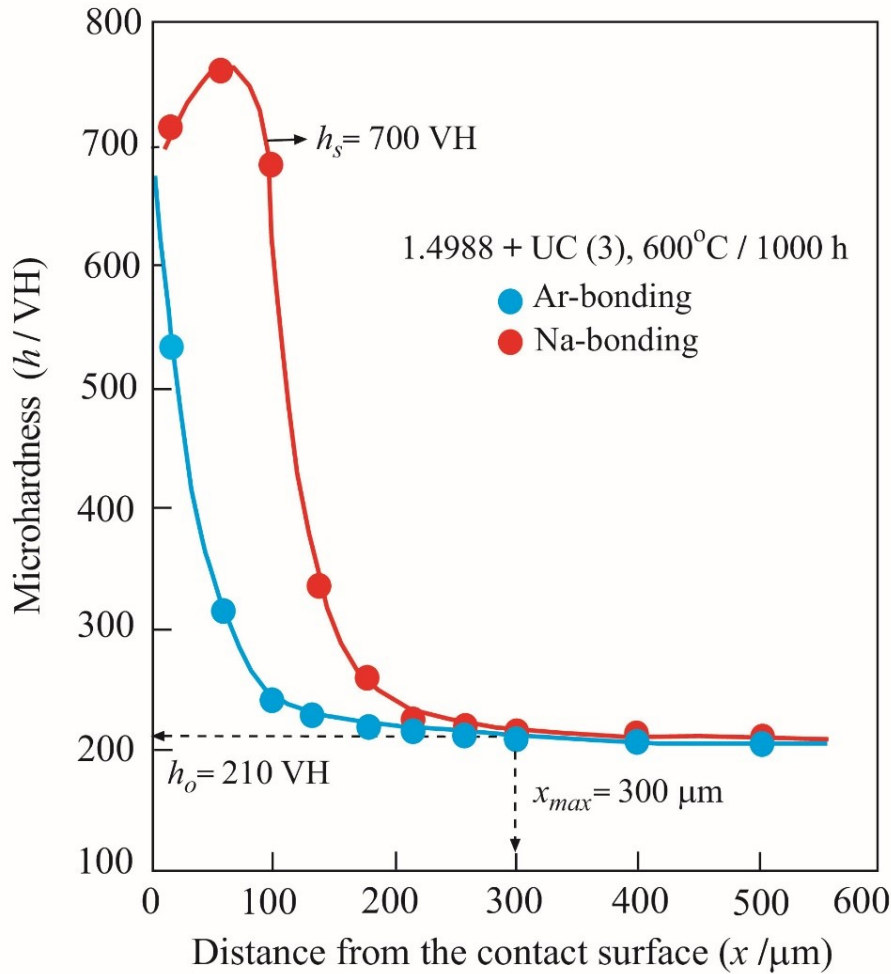


Figure 6: Microhardness profiles for the specimens carburized in UC(3) by Ar-bonding and Na-bonding.

Maximum Hardness and Carburizing Depth

The microhardness profiles revealed that the maximum hardness (h_s) at the contact surface depends on the bonding materials but not the depth (x_{max}) of the carburized zone. The variation of h_s and x_{max} with the mass percent of carbon in the steel was given in Table 2 and represented in Figure 7. The changes in h_s and x_{max} are linear by Ar-bonding, whereas curvilinear by Na-bonding. Consequently, the carbon content in steel has a great effect on the carburizing processes.

Mechanical Properties

The changes in elongation percent, 0.2% yield strength, and tensile strength with increasing carbon content in the uranium carbide powder were given in Table 2 and represented in Figure 8, Figure 9, and Figure 10. The elongation decreases with the carbon content while the 0.2% yield stress and tensile stress increase. These changes are thought to be caused by free carbon atoms in the powders and dissolution of them in Na. The increase in the tensile stress would facilitate the steel cladding process, while a decrease in the elongation percent slows it down. These results are also consistent with the increasing carbon content of steel.

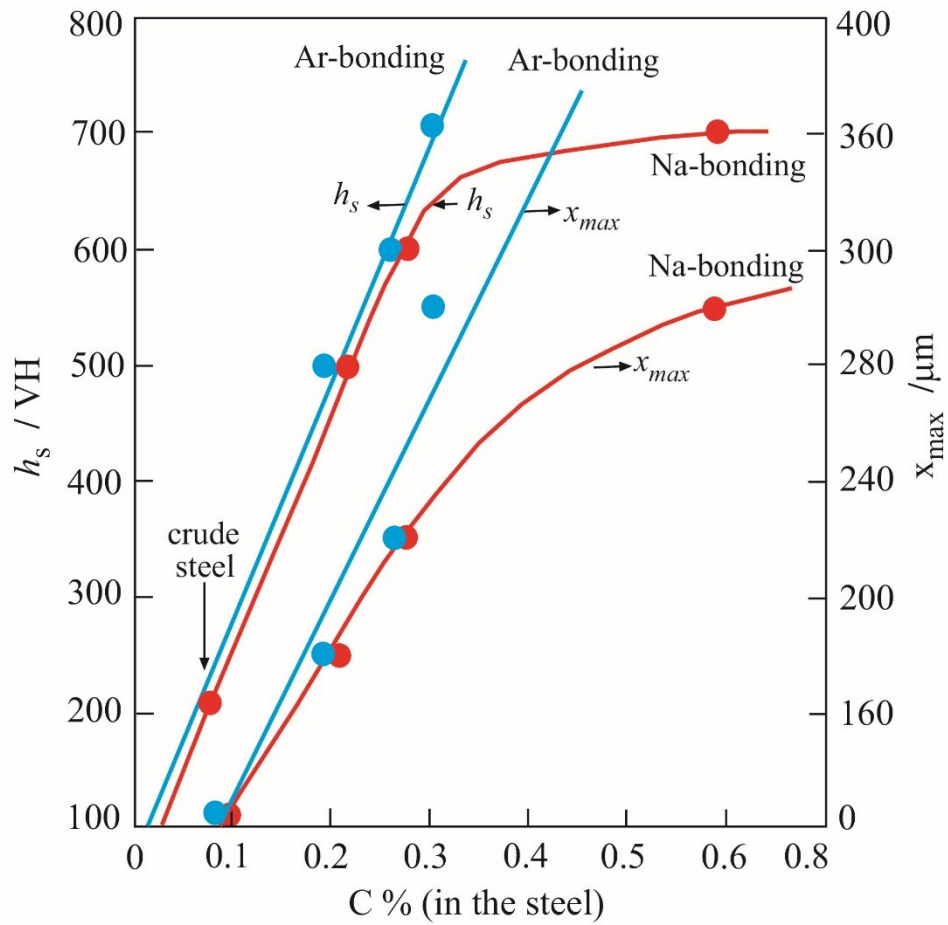


Figure 7: Change in the maximum microhardness (h_s) and maximum depth (x_m) for carburized zone depending on the carbon content in the uranium carbide powder.

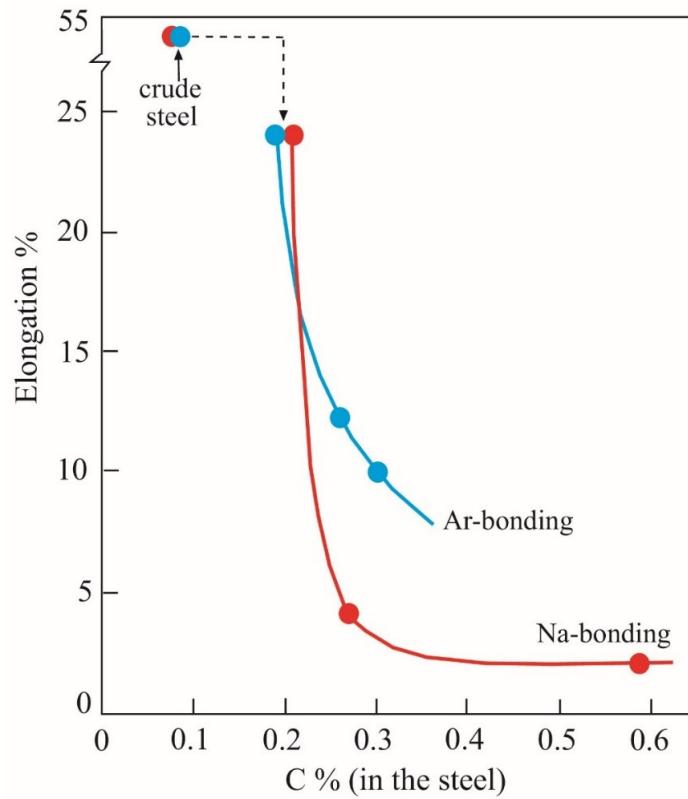


Figure 8: Decreasing of the elongation percent with the carbon content in the steel.

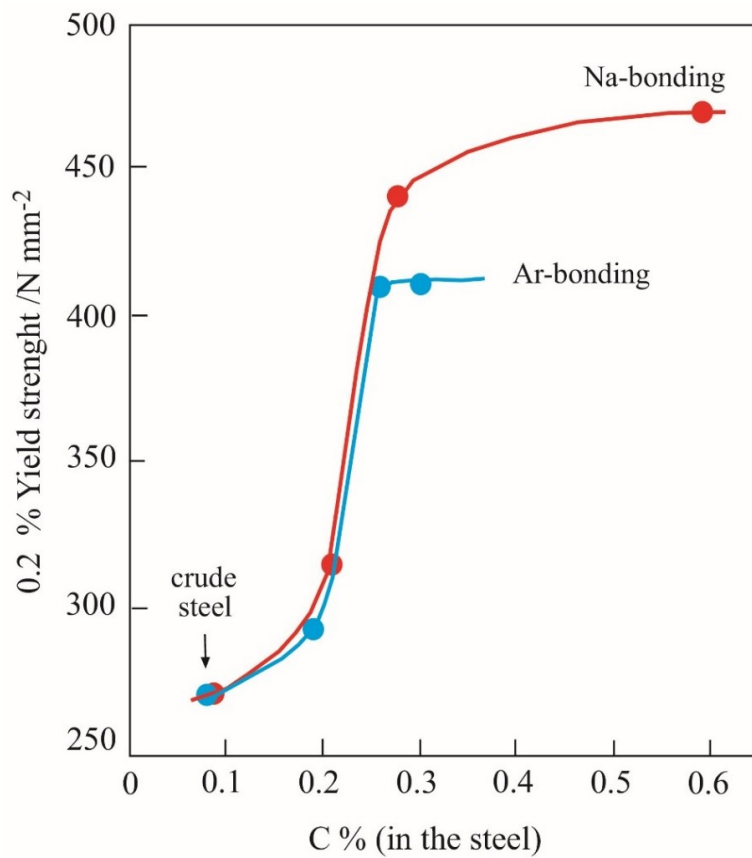


Figure 9: Increasing of the 0.2% yield strength with the carbon content in the steel.

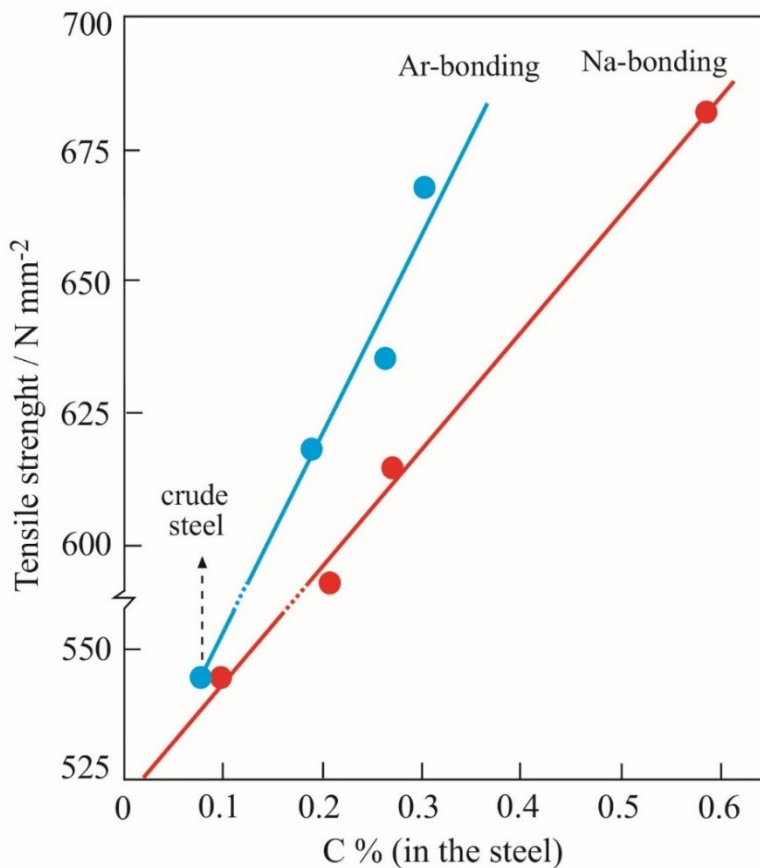


Figure 10: The tensile strength and carbon content in steel.

CONCLUSION

The mechanical properties of steel depend on the physicochemical processes such as the chemical composition of the steel, carburizer, bonding materials, ration of Fe, C, and Fe₃C phases, crystal structure of Fe, heating temperature, and heating and cooling rate. Here, we investigated only the chemical composition of uranium carbide using a carburizer and bonding properties during carburizing of the cladding. Stainless steels was often used as a cladding material for nuclear fuel. The most dangerous nuclear accidents are due to the nuclear fuel and the leakage of the fission products through corroded cladding. Therefore, the corrosion of the cladding materials in contact with nuclear fuels and the fission products at the working temperature of the nuclear reactor should be investigated extensively. Since the chemical properties are similar, non-radioactive materials were used instead of radioactive ones during the experiments. Optimum life of claddings at the high operation temperature of the nuclear reactor was determined according to the effect of corrosion on the mechanical properties such as hardness, elongation, yield stress, and tensile stress. It was determined that bonding characteristics like Ar and Na, in addition to chemical impurities like graphite in uranium carbide, had an impact on the corrosion of the steel.

CONFLICT OF INTEREST

The authors declare that they have no known competing financial interests or personal relationships that could have appeared to influence the work reported in this paper.

ACKNOWLEDGMENTS

We are grateful to Karlsruhe University for experimental facilities and Ankara University Scientific Research Projects Coordination Unit (Project No: 16L043013) for the financial support of this work.

REFERENCES

1. Majumdar S, Sengupta AK, Kamath HS. Fabrication, characterization and property evaluation of mixed carbide fuels for a test Fast Breeder Reactor. *J Nucl Mater.* 2006;352(1-3):165-73. [<DOI>](#)
2. Yan MF. Study on absorption and transport of carbon in steel during gas carburizing with rare-earth addition. *Mater Chem Phys.* 2001;70(2):242-4. [<URL>](#)
3. Farfan S. High cycle fatigue, low cycle fatigue and failure modes of a carburized steel. *Int J Fatigue.* 2004;26(6):673-8. doi:10.1016/j.ijfatigue.2003.08.022 [<DOI>](#)

4. Yao J, Zhang Q, Gao M, Zhang W. Microstructure and wear property of carbon nanotube carburizing carbon steel by laser surface remelting. *Appl Surf Sci.* 2008;254(21):7092-7. [<DOI>](#)
5. Pertek A, Kulka M. Microstructure and properties of composite (B + C) diffusion layers on low-carbon steel. *J Mater Sci.* 2003;38:269-73. [<URL>](#)
6. Wang J, Tao Q, Fu L, Lai W, Shen C, Sun Z, vd. Greater diffusion rate of carbon atoms from nonlinear migration in micro-cell and spatially heterogeneous stable states in FCC iron. *J Mater Sci.* 2018;53(23):15952-68. [<DOI>](#)
7. Pertek A, Kulka M. Characterization of complex (B + C) diffusion layers formed on chromium and nickel-based low-carbon steel. *Appl Surf Sci.* 2002;202:252-60. [<DOI>](#)
8. Sun Y. Kinetics of low temperature plasma carburizing of austenitic stainless steels. *J Mater Process Technol.* 2005;168(2):189-94. [<DOI>](#)
9. Balachandran G, Vadiraj A, Sharath BS, Krishnamurthy BR. Studies on induction hardening of gray iron and ductile iron. *Trans Indian Inst Met.* 2010;63(4):707-13. [<DOI>](#)
10. Dong M, Cui X, Jin G, Wang H, Cai Z, Song S. Improved microstructure and properties of 12Cr2Ni4A alloy steel by vacuum carburization and Ti + N co-implantation. *Appl Surf Sci.* 2018;440:660-8. [<DOI>](#)
11. Gençoğlu S, Yazıcı A. Surface Characteristics and distortion analysis of the case-hardened helical gears: a comparison of different case-hardening treatments. *Trans Indian Inst Met.* 2020;73(1):119-26. [<DOI>](#)
12. Kulka M, Pertek A. Characterization of complex (B + C + N) diffusion layers formed on chromium and nickel-based low-carbon steel. *Appl Surf Sci.* 2003;218(1-4):114-23. [<DOI>](#)
13. Scheuer CJ, Cardoso RP, Mafra M, Brunatto SF. AISI 420 martensitic stainless steel low-temperature plasma assisted carburizing kinetics. *Surf Coat Technol.* 2013;214:30-7. [<URL>](#)
14. Sarıkaya Y, Önal M. High temperature carburizing of a stainless steel with uranium carbide. *J Alloys Compd.* 2012;542:253-6. [<DOI>](#)
15. Çavuşlu F, Usta M. Kinetics and mechanical study of plasma electrolytic carburizing for pure iron. *Appl Surf Sci.* 2011;257(9):4014-20. [<DOI>](#)
16. Sarıkaya Y, Önal M, Pekdemir AD. Application of diffusion and transition state theories on the carburizing of steel AISI 316 by annealing in uranium carbide powder. *Heliyon.* 2019;5(8):e02305. [<DOI>](#)
17. Akita M, Tokaji K. Effect of carburizing on notch fatigue behaviour in AISI 316 austenitic stainless steel. *Surf Coat Technol.* 2006;200(20-21):6073-8. [<DOI>](#)
18. Xia X, Idemitsu K, Arima T, Inagaki Y, Ishidera T, Kurosawa S, vd. Corrosion of carbon steel in compacted bentonite and its effect on neptunium diffusion under reducing condition. *Appl Clay Sci.* 2005;28(1-4):89-100. [<DOI>](#)
19. Panda RR, Mohanty DAM, Mohanta DK. Mechanical and wear properties of carburized low carbon steel samples. *J Multidiscip Curr Res.* 2014; Jan/Feb:109-12. [<URL>](#)
20. Savaria V, Monajati H, Bridier F, Bocher P. Measurement and correction of residual stress gradients in aeronautical gears after various induction surface hardening treatments. *J Mater Process Technol.* 2015;220:113-23. [<DOI>](#)
21. Shen S, Song X, Li Q, Li X, Zhu R, Yang G. Effect of CrxCy-NiCr coating on the hydrogen embrittlement of 17-4 PH stainless steel using the smooth bar tensile test. *J Mater Sci.* 2019;54(9):7356-68. [<DOI>](#)
22. Elangeswaran C, Cutolo A, Muralidharan GK, de Formanoir C, Berto F, Vanmeensel K, et al. Effect of post-treatments on the fatigue behaviour of 316L stainless steel manufactured by laser powder bed fusion. *Int J Fatigue.* 2019;123:31-9. [<DOI>](#)
23. Chen Q-Y, Ren J-K, Xie Z-L, Zhang W-N, Chen J, Liu Z-Y. Correlation between reversed austenite and mechanical properties in a low Ni steel treated by ultra-fast cooling, intercritical quenching and tempering. *J Mater Sci.* 2020;55(4):1840-53. [<DOI>](#)
24. Tian Z, Zhao Y, Jiang Y, Ren H, Qin C. Investigation of microstructure and properties of FeCoCrNiAlMox alloy coatings prepared by broadband-beam laser cladding technology. *J Mater Sci.* 2020;55(10):4478-92. [<DOI>](#)
25. Sahu JN, Sasikumar C. Mechanical properties of a Ni-Cr-Mo steel subjected to room temperature carburizing using surface mechano-chemical carburizing treatment (SMCT). *Trans Indian Inst Met.* Nisan 2018;71(4):915-21. [<DOI>](#)
26. Sahu JN, Sasikumar C. Evaluation of microstructure due to addition of carbon in Ni-Cr-Mo steel mechanically through surface mechanochemical case carburizing treatment (SMCT). *Trans Indian Inst Met.* 2019;72(1):55-63. [<DOI>](#)
27. Zhang W, Fang K, Hu Y, Wang S, Wang X. Effect of machining-induced surface residual stress on initiation of stress corrosion cracking in 316 austenitic stainless steel. *Corros Sci.* 2016;108:173-84. [<DOI>](#)
28. Wang S, Hu Y, Fang K, Zhang W, Wang X. Effect of surface machining on the corrosion behaviour of 316 austenitic stainless steel in simulated PWR water. *Corros Sci.* 2017;126:104-20. [<DOI>](#)
29. Yang Y, Yan MF, Zhang YX. Tribological behavior of diamond-like carbon in-situ formed on Fe₃C-containing carburized layer by plasma carburizing. *Appl Surf Sci.* 2019;479:482-8. [<DOI>](#)
30. Sahu JN, Sasikumar C. Room Temperature case carburizing of a Ni-Cr-Mo steel through shot peening/blasting techniques. *Trans Indian Inst Met.* 2015;68(S2):227-33. [<DOI>](#)
31. Yang Y, Yan MF, Zhang SD, Guo JH, Jiang SS, Li DY. Diffusion behavior of carbon and its hardening effect on plasma carburized M50NiL steel: Influences of treatment temperature and duration. *Surf Coat Technol.* 2018;333:96-103. [<DOI>](#)
32. Argade GR, Shukla S, Liu K, Mishra RS. Friction stir lap welding of stainless steel and plain carbon steel to enhance corrosion properties. *J Mater Process Technol.* 2018;259:259-69. [<DOI>](#)
33. Ozturk B, Fearing VL, Ruth JA, Simkovich G. Self-diffusion coefficients of carbon in F₃C at 723 K via the

kinetics of formation of this compound. Metall. Mater. Trans. 1982;13A:1871-73. [<URL>](#)

34. Ahamad NW, Jauhari I, Azis SAA, Aziz NHA. Kinetics of carburizing of duplex stainless steel (DSS) by superplastic compression at different strain rates. Mater Sci Eng A. 2010;527(16-17):4257-61. [<DOI>](#)

35. Yang Y, Yan MF, Zhang YX, Li DY, Zhang CS, Zhu YD, vd. Catalytic growth of diamond-like carbon on Fe₃C-containing carburized layer through a single-step plasma-assisted carburizing process. Carbon. 2017;122:1-8. doi.org/10.1016/j.carbon.2017.06.033 [<DOI>](#)

36. Cao Z, Liu T, Yu F, Cao W, Zhang X, Weng Y. Carburization induced extra-long rolling contact fatigue life of high carbon bearing steel. Int J Fatigue. 2020;131:105351. [<DOI>](#)

